

Optimization of structural and optical properties of $\text{CuIn}_{1-x}\text{Zn}_x\text{Se}_2$ thin films by zinc incorporation

K. BENAMEUR¹, Y. MOUCHAAL^{1,2,*}, B. KOUSKOUSA¹, A. TAB³, K. EL ASSAD ZEMALLACH OUARI^{1,2}, E. EL-MENYAWY⁴, K. BENCHOUK¹, K. ABDELBA CET¹

¹Laboratoire de Physique des Couches Minces et Matériaux pour L'Electronique (LPCMME), Université Oran 1 Ahmed Ben Bella, BP 1524 Oran El-Mnaouer, Algeria

²Département de Physique, Faculté des Sciences Exactes, Université Mustapha Stambouli de Mascara, B.P. 305, Mascara 29000, Algeria

³Physics Department, Science Faculty, Oran University of Sciences and Technology USTO-MB, BP1505 Oran, Algeria

⁴Solid State Electronics Laboratory, Solid State Physics Department, Physics Research Division, National Research Centre, 33 El-Bohouth St., Dokki, Giza 12622, Egypt

In the present work, we investigate on the effect of incorporating zinc into $\text{CuIn}_{1-x}\text{Zn}_x\text{Se}_2$ thin layer structures aiming to improve its optoelectronic performances towards application as active layers in thin layers photovoltaic cells. During this work, we have shown that the atomic percentage of Zn in the $\text{CuIn}_{1-x}\text{Zn}_x\text{Se}_2$ thin films influences the structural, optical and morphological properties of the produced layers. $\text{CuIn}_{1-x}\text{Zn}_x\text{Se}_2$ films with various zinc compositions were synthesized by in situ annealing of Cu/In/Zn/Se multilayers after sequential deposition of Cu, In, Zn and Se thin films on unheated glass substrates using thermal evaporation method. Thermal annealing was carried out using halogen lamp under vacuum at 10^{-4} Pa. The chalcopyrite phase, polycrystalline nature, film homogeneity and stoichiometry were illustrated and studied using appropriate analysis. The grain size had a decreasing behavior from 120 nm to 40 nm with increasing zinc percentage. Optical study showed electronic energy gap values of $\text{CuIn}_{1-x}\text{Zn}_x\text{Se}_2$ compounds increases from 1.15 eV to 1.75 eV with the increase in the molar fraction of zinc. The results carried in this study demonstrated that zinc can be an effective candidate for In substitution in chalcopyrite structures with an effect similar to gallium and aluminum aiming to reduce the cost and to adjust the energy gap by adapting the In / Zn atomic ratio which permit to optimize the absorption of the solar spectrum.

(Received May 20, 2021; accepted February 11, 2022)

Keywords: $\text{CuIn}_{1-x}\text{Zn}_x\text{Se}_2$, Chalcopyrite structures, Sequential deposition, Photovoltaic cells

1. Introduction

Nowadays thin-film solar cells based on chalcopyrite materials such as CuInSe_2 [1], CuGaSe_2 [2], Cu(In, Ga)Se_2 [3], CuInAlSe_2 [4] have a particular interest due to their easy manufacturing, cost-reduction potential, stability, flexibility and aesthetic design options [5]. This quality of solar cells largely depends on the choice of material used to make the absorbent layer enabling using light rays for generating free electrical charges. For this, copper and indium selenide (CuInSe_2) is a good promising candidate for absorbent materials in thin film photovoltaic devices due to its good thermal stability, its direct gap of around $E_g = 1.04$ eV, and of their high absorption coefficient 105cm^{-1} [6]. One of the major challenges in photovoltaic devices based on this material is the existence of indium. Unlike copper, indium is a rare metal on earth, which constitutes an obstacle to the development of new materials such as CuInSe_2 . This led us to look for other materials that provide improved performance for application in the photovoltaic field.

Our objective is to optimize a new absorber compound similar to CuInSe_2 in thin layer by substituting indium with another abundant and less expensive element like zinc allowing to manufacture a thin film solar cell with a high open circuit voltage (V_{OC}) and low cost. This

new compound is $\text{CuIn}_{1-x}\text{Zn}_x\text{Se}_2$ (CIZS) which offers the advantage of adapting the appropriate values of the network parameters and the band gap energy [7]. In addition, permits achieving a sufficient energy conversion efficiency to compete with the more developed thin film technologies [5]. This quaternary compound can be synthesized by several techniques such as sputtering [8], spray pyrolysis [9], RF-sputtering [10] and DC magnetron [11]. In this study, we synthesized $\text{CuIn}_{1-x}\text{Zn}_x\text{Se}_2$ films with different percentage of zinc by in-situ annealing of Zn / In / Cu / In / Zn / Se sequential deposited structure using thermal evaporation. Then, by characterizing their crystalline and optical properties by XRD, EDX, SEM, AFM, XPS and UV-visible we studied the influences of Zn percentage in composition and opto-electrical properties of the obtained microstructures.

2. Experimental details

2.1. Films preparation

For chalcopyrite structures deposition we used as substrate microscopic glass cleaned with soap, acetone, ethanol and rinsed with distilled water then they were introduced after drying in the vacuum chamber. For the sequential deposition of metals we used as deposit source,

metallic elements (99.99% Sigma Aldrich), three tungsten crucibles for the deposition of copper, zinc and selenium and a molybdenum crucible for the deposition of indium.

The $\text{CuIn}_{1-x}\text{Zn}_x\text{Se}_2$ polycrystalline structures with different zinc compositions were deposited as schematized in figure 1 by sequential thermal evaporation of the Zn / In / Cu / Se layers in the appropriate atomic ratio under vacuum 7.10^{-4} Pa where the number of layers was 4, 4, 3 and 1 for Zn, In, Cu and Se respectively. The thickness and deposition rate of the individual layers were checked in-situ using a quartz microbalance. A detail on the

thicknesses and deposition rates of the various elements is detailed in Table 1.

After the sequential deposition by successive layers according to this chosen configuration, the metal alloy has undergone an in-situ thermal annealing by halogen lamps under vacuum 10^{-3} Pa at a temperature of 350°C for 30 min in order to synthesize $\text{CuIn}_{1-x}\text{Zn}_x\text{Se}_2$ alloy layers. The total thickness of the $\text{CuIn}_{1-x}\text{Zn}_x\text{Se}_2$ films is measured by Dektak XT stylus profiler having an order of 400 nm and 600 nm respectively.

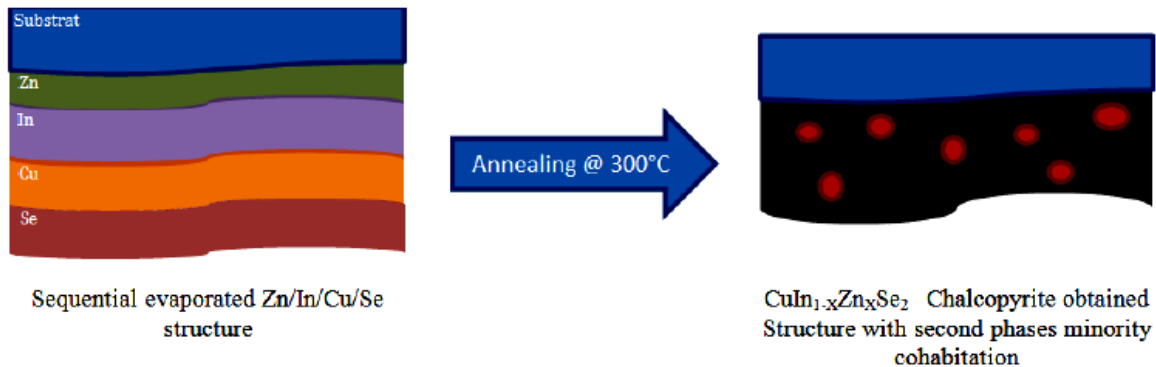


Fig. 1. $\text{CuIn}_{1-x}\text{Zn}_x\text{Se}_2$ structures preparation by thermal evaporation root (color online)

Table 1. Deposition conditions of CIZS structures

Samples	CIS			CIZS1				CIZS2			
	Cu	In	Se	Cu	In	Zn	Se	Cu	In	Zn	Se
Thickness (nm)	121.2	268.5	556.8	121.2	252.4	9.40	556.8	121.2	239.0	17.2	556.8
Deposition rate ($\text{\AA}/\text{s}$)	0.9-1.2	0.9-1.6	0.9-3.0	0.9-1.2	0.9-1.6	0.9-1.6	0.9-3.0	0.9-1.2	0.9-1.6	0.9-1.6	0.9-3.0

2. Thin films characterization

CIZS thin films structural characterizations were identified by X-ray Siemens D5000 diffractometer using Cu $K\alpha$ radiation ($\lambda = 1.54056\text{\AA}$). Morphology, homogeneity and surface composition were observed by SEM (JEM JEOL 7600F) and AFM microscope (NT-MDT model BL222RNTE). Composition analysis was performed using EDX (combined to SEM) and XPS (Nova analytical Spectrometer, Kratos). Optical parameters were determined using a UV-visible Perkin spectrophotometer in the wavelength range of 400 to 1200 nm at room temperature.

3. Results and discussion

3.1. Structural properties

Structural properties of $\text{CuIn}_{1-x}\text{Zn}_x\text{Se}_2$ have been characterized by XRD analysis obtained by in-situ annealing of sequentially deposited In, Zn, Cu and Se layers are presented in Fig. 2.

The XRD diagrams show that the films are well crystallized. They have well-defined peaks corresponding to (112), (220), (312), (400), (332) and (228) and low intensity peaks (101), (103) and (211) confirming the chalcopyrite phase of the deposited compounds. The crystallization of the films is oriented towards the main most intense peak corresponding to the (112) planes. Fig. 1 clearly shows that the intensity of the diminished peaks and the (101) and (211) peaks of the chalcopyrite phase tend to disappear with the increase of the zinc content in the CIZS films [12], therefore the tetragonal phase is well formed in our structures when the zinc content is lower. In addition, no significant shift in the peak positions was detected by the insertion of Zn [9].

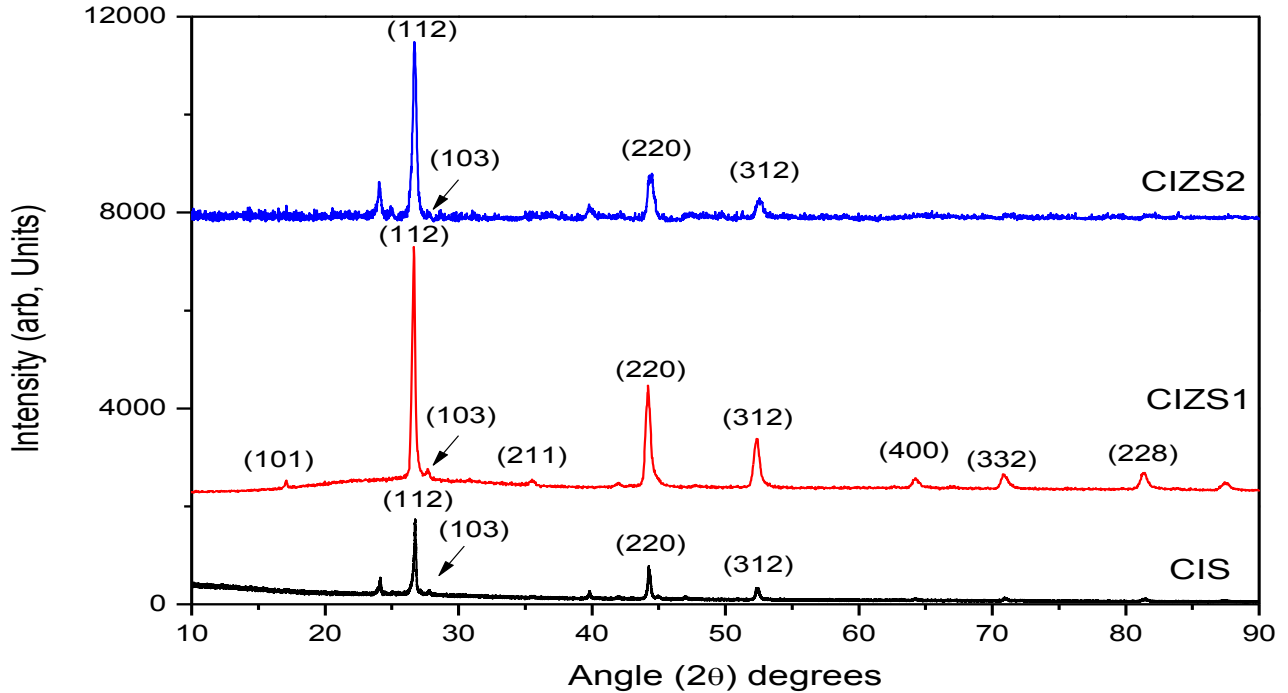


Fig. 1. XRD patterns of $\text{CuIn}_{1-x}\text{Zn}_x\text{Se}_2$ thin films (color online)

In order to observe more closely the effect of the incorporation of zinc in CIZS structures, we group in Table 2 the lattice parameters “a” and “c” calculated using Bragg's law (equation 1) and inter-reticular distance of the tetragonal structure of the two (112) and (103) successive peaks (equation 2).

$$2d_{hkl} \sin\theta = n\lambda \quad (1)$$

$$\frac{1}{d} = \frac{h^2 + k^2}{a^2} + \frac{l^2}{c^2} \quad (2)$$

We note from structural analysis results that the “c/a” ratio of crystal lattice decreases when the content of zinc increases in the CIZS compounds. This may be due to the fact that the size of the zinc atom is smaller than that of

indium and therefore causes a shrinking of the network during the substitution of indium sites in the cell [13]. The grain size average of the deposited films was determined from the X-ray diffraction diagram using Scherrer's formula, expressed by $D = K\lambda / \beta \cos\theta$, where K is a structure factor equal to 0.94, λ being the X-ray wavelength, β being defined as full width half maximum value (FWHM), and θ is the X rays diffraction angle. We have noted from the grain sizes values represented in Table 2 that for CIS compounds the grain size is larger than that of CIZS films. We have also noticed that the decrease in the grain size in CIZS is followed by an increase in the grain size in film, probably due to the role of zinc as an additional nucleation site, which improves nucleation therefore increase in grain boundaries [10]. These findings will be confirmed by SEM analyzes.

Table 2. Structural parameters of $\text{CuIn}_{1-x}\text{Zn}_x\text{Se}_2$ thin films

Samples	a (Å)	c (Å)	c/a	D (nm)
CIS	5.760	11.570	2.008	120.6
CIZS1	5.784	11.609	2.007	47.15
CIZS2	5.773	11.565	2.003	40.8

3.2. Morphological and composition analysis

The scanning electron microscope was used to visualize the surfaces microstructures and its combined EDX analysis to determine the composition of the CIS and CIZS films.

The total content of CIS and CIZS structures in Cu, In, Zn and Se presented in Table 3 reveals that the atomic

percentage of selenium and copper is almost constant for CIZS films but the atomic percentage of indium decreases by increasing in zinc concentration in the deposited films. These results show that the decrease in indium in CIZS films is due to an anti-site substitution of zinc at the sites of indium in the chalcopyrite compounds [10].

Table 3. EDX composition of CIS and CIZS thin films

Sample	Composition (%)				Cu/(In+Zn)	Zn/In
	Cu	In	Zn	Se		
CIS	32.00	22.00	-	45.00	1.45	-
CIZS 1	28.97	19.55	5.67	45.81	1.14	0.29
CIZS 2	29.35	14.63	10.92	45.09	1.14	0.74

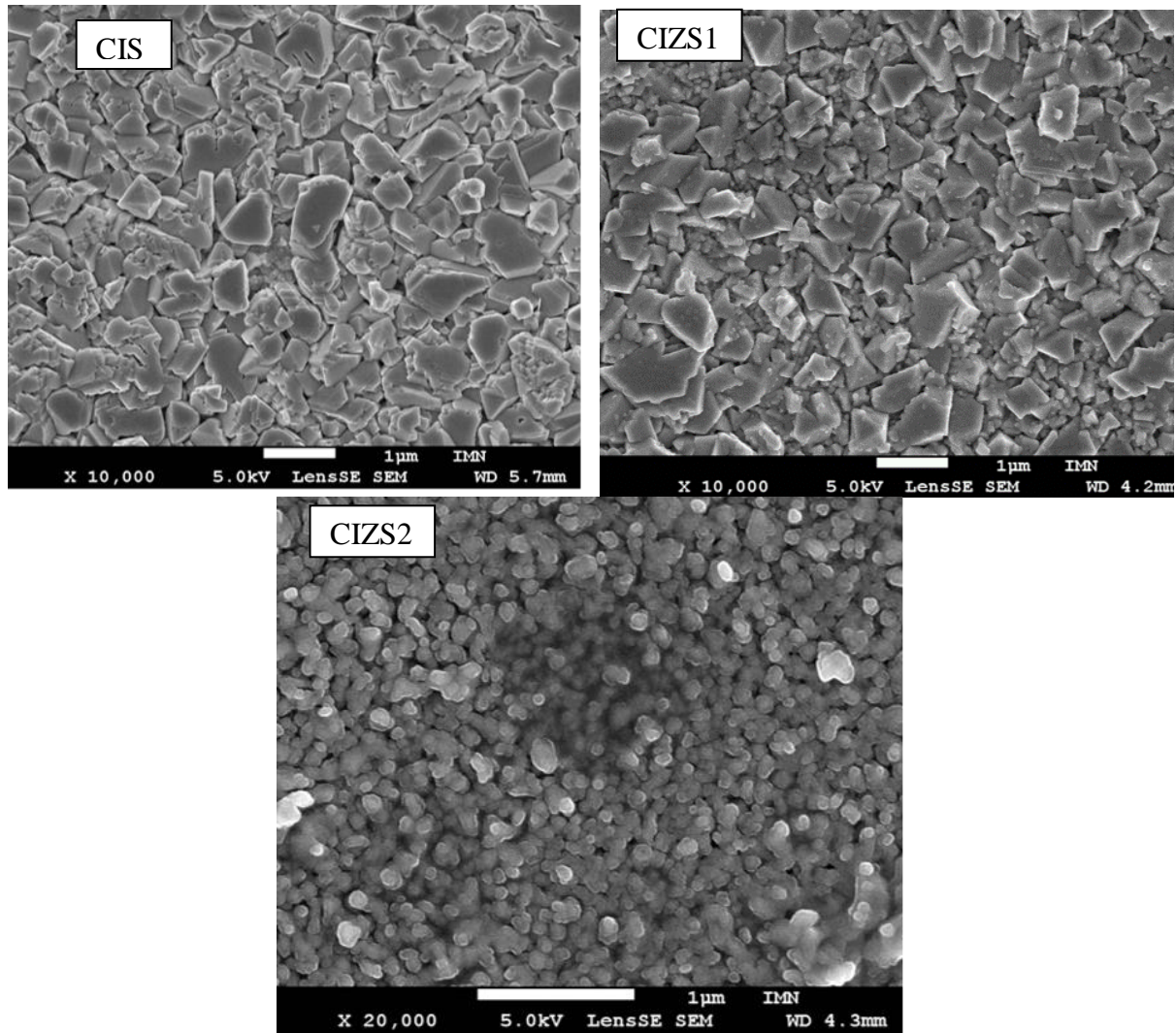


Fig. 3. SEM images of CIS and CIZS thin films

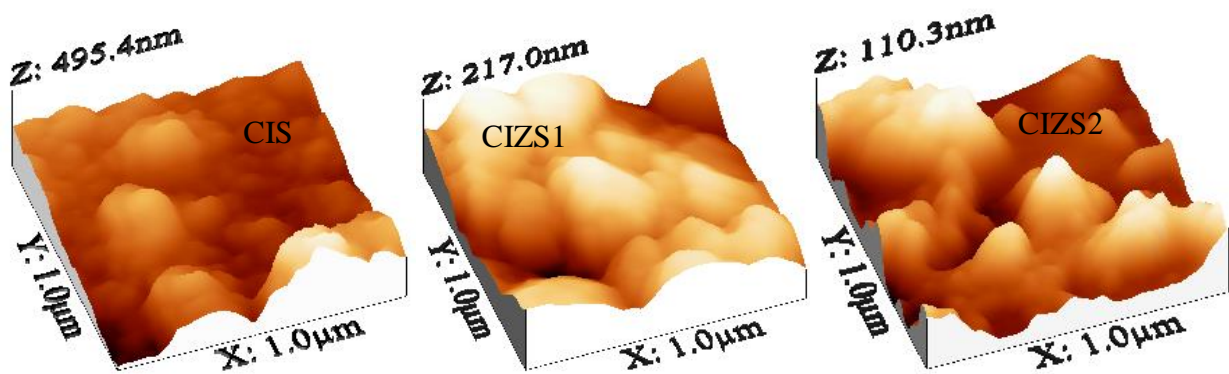


Fig. 4. AFM images of CIS and CIZS thin films (color online)

The visualization of CIS and CIZS thin layers surfaces by SEM presented in Fig. 3 shows that the deposited films have almost good homogeneity and distribution on the substrate. The layers are polycrystalline with well-defined, clearly visible, compact, dense and homogeneous grains. We can also see that there is a marked influence on the morphology of the surface when the atomic concentration of zinc has increased. Increasing the zinc concentration in the films decreases the grain size. Smaller grain size lead to increase in grain boundaries and to grain boundary potentials [14] causing an increase in the recombination rate of photo-generated electrons in solar cells which is detrimental to the efficiency of the photovoltaic device [15].

The effect of zinc atomic percentage on the topology of synthesized films was studied by AFM analyzes of the CIS and CIZS films surfaces. The AFM images illustrated in Fig. 4 show that the surface grains have triangular shape. This form is very advantageous for the upper layers in the solar cells which permit to reduce the photonic loss by reflection of the incident beam and improves the trapping of light in the solar cells [16].

The surface roughness values of the CIS, CIZS1 and CIZS2 films are 75, 42 and 23 nm respectively. Furthermore, this analyzes also showed that the roughness of studied films decreases with the increase in the atomic ratio of Zn/In due to the fact that the smallest grains have lower roughness [17]. This result is in good agreement similar studies on CIZS compounds [18,19] and that obtained in the case of CIGS [17, 20] and CIAISe [21]. We note from the CIZS1 film images that they present a more compact surface with a better morphology which allows better contact formation of junction basing on the fact that for films with systematically low roughness tend generally to reduce the dark current and the density of interface states which is essential for the production of a high performance solar cell [22, 23].

3.3. Optical properties

Optical absorbance measurements of CIS and CIZS thin films in the [400-1100nm] range were performed at room temperature as a function of the wavelength in order to determine the optical properties of deposited thin films.

The UV-Vis (Fig. 5) absorbance spectrum of CIS and CIZS films shows a wide absorption in the visible region, indicating their absorbency of the visible optical light [9]. The $\text{CuIn}_{1-x}\text{Zn}_x\text{Se}_2$ chalcopyrite is a direct band gap semiconductor, so to determine optical band gap films, we extrapolate to zero the linear part of the curve representing $(\alpha h\nu)^2=f(h\nu)$ function illustrated in Fig. 5.

We note from measured optical parameters of CIZS thin films (Table 4) that the band gap increases by increasing the zinc molar fraction because the presence of zinc in the CIZS thin layer modifies the cation-anion bond leading to an increase of the band gap of the film [24].

Table 4. Optical properties of CIS and CIZS thin films

Sample	Zn/In	Band Gap (eV)
CIS	-	1.15
CIZS1	0.29	1.40
CIZS2	0.74	1.75

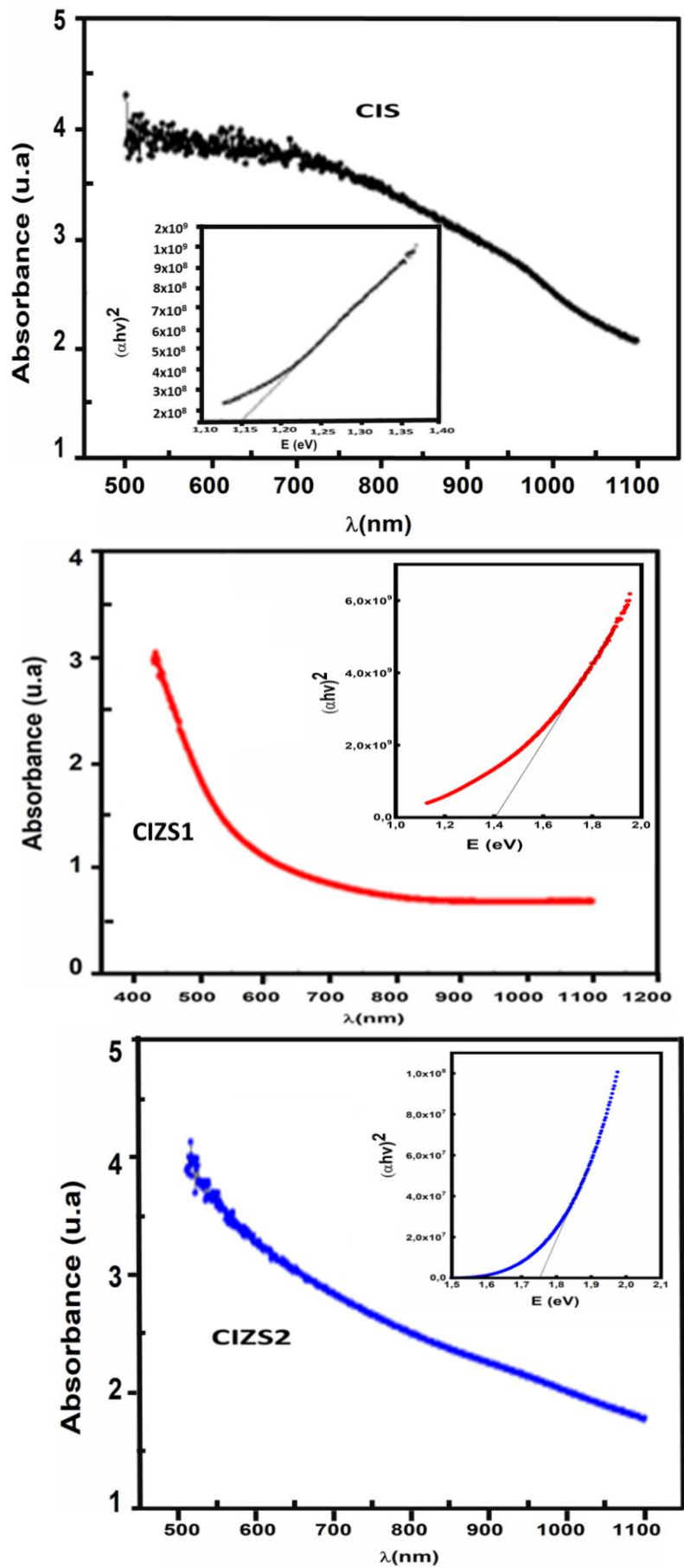


Fig. 5. Absorption spectra and Plot of $(\alpha h\nu)^2$ curve versus incident light energy of CIS and CIZS thin films (color online)

4. Conclusion

We showed in this study that the atomic percentage of zinc strongly influences the structural and optical properties of CuIn_{1-x}Zn_xSe₂-based chalcopyrite compounds thin films prepared by thermal evaporation root. Analysis by XRD confirmed that the films are crystallized in the chalcopyrite structure, which makes them promising candidates for possible effective application in thin film solar cells with better photovoltaic conversion efficiency. It also shows that the volume of the elementary mesh decreases with the increase in the molar fraction of zinc. Furthermore, the photographs obtained by SEM and AFM have shown that the grain size decreases with the increase in zinc. The layers obtained also have interesting optical properties. Optical measurements revealed a slight increase in the band gap energy with the increase in the molar fraction of zinc in of CuIn_{1-x}Zn_xSe₂ films.

Acknowledgments

The authors acknowledge the funding granted by the Algerian Ministry of Higher Education and Scientific Research (MESRS) as well as the General Direction of Scientific Research and Scientific Development (DGRSDT).

Pr. K. Benchouk and Dr. K. Benameur would like to thank Pr M. Ghamnia from Oran 1 University, Algeria, for AFM Analysis.

References

- [1] K. Liu, Y. Xu, Q. Sun, H. Li, H. Wu, *Results in Physics* **12**, 766 (2019).
- [2] G. Yin, C. Merschjann, M. Schmid, *Journal of Applied Physics* **113**, 213510 (2013).
- [3] T. K. Todorov, D. M. Bishop, Y. S. Lee, *Solar Energy Materials and Solar Cells* **180**, 350 (2018).
- [4] Y. Ganjkanlou, T. Ebadzadeh, M. Kazemzad, A. Maghsoudipour, M. Keyanpour-Rad, *Advanced Ceramics Progress* **2**, 1 (2016).
- [5] R. Kondrotas, M. Colina, M. Guc, M. Neuschitzer, S. Giraldo, X. Alcobé, F. Oliva, Y. Sánchez, P. Pistor, V. Izquierdo-Roca, A. Pérez-Rodríguez, E. Saucedo, *Solar Energy Materials and Solar Cells* **160**, 26 (2017).
- [6] I. J. Choi, J. W. Jang, S. M. Lee, D. H. Yeon, Y. H. Jo, M. H. Lee, J. H. Yun, K. H. Yoon, Y. S. Cho, *J. Phys. D: Appl. Phys.* **46**, 245102 (2013).
- [7] V. F. Gremenok, E. P. Zaretskaya, V. M. Siarheeva, K. Bente, W. Schmitz, V. B. Zalesski, H. J. Möller, *Thin Solid Films* **487**, 193 (2005).
- [8] H. H. Güllü, M. Parlak, *J. Semicond.* **38**, 123001 (2017).
- [9] A. H. Cheshme Khavar, A. R. Mahjoub, N. Taghavinia, *J. Phys. D: Appl. Phys.* **50**, 485103 (2017).
- [10] R. A. Wibowo, K. H. Kim, *Solar Energy Materials and Solar Cells* **93**, 941 (2009).
- [11] M. Guc, F. Oliva, R. Kondrotas, X. Alcobe, M. Placidi, P. Pistor, E. Saucedo, A. Perez-Rodriguez, V. Izquierdo-Roca, *Prog. Photovolt. Res. Appl.*, 3150 (2019).
- [12] K. Takei, T. Maeda, F. Gao, S. Yamazoe, T. Wada, *J. Appl. Phys.* **53**, 1 (2014).
- [13] M. Venkatachalam, M. D. Kannan, S. Jayakumar, R. Balasundaraprabhu, N. Muthukumarasamy, *Thin Solid Films* **516**, 6848 (2008).
- [14] K. G. Deepa, R. Jayakrishnan, K. P. Vijayakumar, C. Sudha Kartha, V. Ganesan, *Solar Energy* **83**, 964 (2009).
- [15] J.-S. Hahn, S.-H. Lee, M.-S. Seo, D.-K. Choi, J. Lee, J. Shim, *Thin Solid Films* **546**, 279 (2013).
- [16] R. Jayakrishnan, P. M. R. Kumar, C. S. Kartha, K. P. Vijayakumar, *Meas. Sci. Technol.* **17**, 3301 (2006).
- [17] B. Peace, J. Claypoole, N. Sun, D. Dwyer, M. D. Eisaman, P. Haldar, H. Efstathiadis, *Journal of Alloys and Compounds* **657**, 873 (2016).
- [18] K.-W. Cheng, W.-C. Lee, M.-S. Fan, *Electrochimica Acta* **87**, 53 (2013).
- [20] S. Jung, S. Ahn, J. H. Yun, J. Gwak, D. Kim, K. Yoon, *Current Applied Physics* **10**, 990 (2010).
- [21] J. López-García, M. Placidi, X. Fontané, V. Izquierdo-Roca, M. Espindola, E. Saucedo, C. Guillén, J. Herrero, A. Pérez-Rodríguez, *Solar Energy Materials and Solar Cells* **132**, 245 (2015).
- [22] L. Li, Y. Ma, G. Gao, W. Wang, S. Guo, J. You, J. Xie, *Journal of Alloys and Compounds* **658**, 774 (2016).
- [23] J. Liu, D. Zhuang, H. Luan, M. Cao, M. Xie, X. Li, *Progress in Natural Science: Materials International* **23**, 133 (2013).
- [24] C. Guillén, J. Herrero, *Journal of Physics and Chemistry of Solids* **72**, 1362 (2011).

*Corresponding author: younes.mouchaal@univ-mascara.dz